

Received June 5, 2016, accepted July 4, 2016, date of publication August 8, 2016, date of current version September 16, 2016.

Digital Object Identifier 10.1109/ACCESS.2016.2590440

Selective Level Set Segmentation Using Fuzzy Region Competition

BING NAN LI¹, (Senior Member, IEEE), JING QIN², RONG WANG³, (Member, IEEE),
MENG WANG⁴, (Member, IEEE), AND XUELONG LI⁵, (Fellow, IEEE)

¹Department of Biomedical Engineering, Hefei University of Technology, Hefei 230009, China

²Center for Smart Health, School of Nursing, The Hong Kong Polytechnic University, Hong Kong

³Xi'an Research Institute of Hi-Tech, Xi'an 710201, China

⁴School of Computer Science and Information Engineering, Hefei University of Technology, Hefei 230009, China

⁵State Key Laboratory of Transient Optics and Photonics, Center for Optical Imagery Analysis and Learning, Xi'an Institute of Optics and Precision Mechanics, Chinese Academy of Sciences, Xi'an 710119, China

Corresponding author: B. N. Li (bingoon@ieee.org)

This work was supported in part by the Anhui Natural Science Foundation under Grant 1608085J04, in part by the International Science and Technology Cooperation Plan of Anhui Province under Grant 1503062015, and in part by the National Natural Science Foundation of China under Grant 61271123, Grant 61511140099, and Grant 61571176.

ABSTRACT Deformable models and level set methods have been extensively investigated for computerized image segmentation. However, medical image segmentation is yet one of open challenges owing to diversified physiology, pathology, and imaging modalities. Existing level set methods suffer from some inherent drawbacks in face of noise, ambiguity, and inhomogeneity. It is also refractory to control level set segmentation that is dependent on image content and evolutional strategies. In this paper, a new level set formulation is proposed by using fuzzy region competition for selective image segmentation. It is able to detect and track the arbitrary combination of selected objects or image components. To the best of our knowledge, this new formulation should be one of the first proposals in a framework of region competition for selective segmentation. Experiments on both synthetic and real images validate its advantages in selective level set segmentation.

INDEX TERMS Fuzzy control, image segmentation, level set methods, region competition, selective segmentation.

I. INTRODUCTION

Segmentation is one of the most essential steps in computer vision and image analysis [1], [2]. A plethora of algorithms have been proposed for this purpose. Techniques based on deformable models are attractive as they can integrate image information (e.g., intensity and gradients) and model properties (e.g., smoothness and curvature) for optimal segmentation [3]. There are two related but different approaches for deformable models, namely active contour models (ACMs) and level set methods (LSMs) [4]. LSMs incorporate the dynamic interfaces implicitly into a higher-dimensional Lipschitz function, where the dynamic interfaces can be recovered by checking the zero level set, and drive interface evolution by means of simple geometric operations [5].

Two level set formulations have been well established for image segmentation. The first one is derived from the Hamilton-Jacobi functional [6] while the second one is based on the Mumford-Shah functional [7]. The Hamilton-Jacobi

level set models (HJ-LSMs), with appropriate initialization and controlling parameters, are able to detect and track local objects. This kind of edge-based LSMs depends on the premise that those objects have a clear and distinct boundary. However, the object indication function is often weak or discontinuous; hence the dynamic interface eventually leaks away [8]. Chan and Vese [9] proposed a Mumford-Shah functional for level set modeling and evolution, which eliminates the object indication function in HJ-LSMs. Cremers et al. [10] have clarified that this kind of region-based LSMs is equivalent to a general statistical formulation, which is flexible to incorporate intensity, color and texture for segmentation. The Mumford-Shan LSMs (MS-LSMs) nonetheless have inherent drawbacks in not being able to detect a specific local object of interest [11].

Both HJ-LSMs and MS-LSMs have been enhanced in a variety of ways for efficient computing and robust evolution. Coming to HJ-LSMs, Taheri et al. [12] proposed to define the

HJ-LSM's speed function by adaptive thresholding and have validated it on brain tumor segmentation. In order to cope with the issue of boundary leakage, Li et al. [8] introduced fuzzy control into the balloon force, which always expands or shrinks till strong boundaries, for bidirectional evolution. Fuzzy logic is a subject that was proposed to tackle the issues of approximation and uncertainty that are common and refractory in medical image analysis [13]. It has been proposed more than once to control LSMs with fuzzy logics in literature [14]. Furthermore, Zhang et al. [11] proposed to regularize the force of region competition with a Gaussian smoothing kernel for signed pressure force, which enabled the shifting between local and global segmentation. This technique was reported again by Dong et al. [15] for boundary enhancement and inhomogeneity suppression. It shed light on the connection of HJ-LSMs and MS-LSMs for unified level set segmentation [16].

In terms of MS-LSMs, they are advantageous for stable evolution and fast convergence, but they are susceptible to image inhomogeneity. Therefore, most attention has been paid in this regard, including region scalable fitting [17] and Gaussian distribution with bias field [18]. Those solutions usually replaced the piecewise constants in MS-LSMs by statistical probability density functions [19]–[21]. For example, a joint probabilistic model that correlated a new probabilistic shape model with the corresponding global intensity distribution was proposed to segment multiple abdominal organs simultaneously [22]. The probabilistic model's controlling parameters were tuned in a Bayesian framework and were trained according to the training datasets. The model of local binary fitting (LBF) by Li et al. [17] is one of the first attempts to cope with field inhomogeneity in MS-LSMs, but it is known sensitive to initialization. Wang et al. [23] proposed an extended structure tensor (EST) by adding the intensity information into the classical structure tensor for texture image segmentation. Rastgarpour et al. [24] proposed a coarse-to-fine framework and took the advantage of suitable parameter selection by using prototype-driven fuzzy local information c-means clustering for inhomogeneous medical image segmentation. Actually, medical imaging usually involves a series of volumetric or temporal scans, whose inter-slice information can be utilized to guide level set segmentation [25].

The general HJ-LSMs and MS-LSMs are capable of binary image segmentation only. Although it has been proved by Vese and Chan [26] that the Mumford-Shan framework is extendable for multiphase level set segmentation, the phase is limited to octave segmentation and the optimization is computationally expensive. In order to alleviate computational costs, Zhan et al. [18] assumed that background was nearly zero and proposed a specially-designed three-phase level set function for brain tissue segmentation. It is also possible to remodel MS-LSM in a statistical framework, and pursue optimal image segmentation in a way of minimization [10]. The latter is nonetheless out of the question in this study.

Different from the existing works, we attempt to propose a new level set model with fuzzy region competition for selective image segmentation. It allows fuzzy control in a couple of ways: first, fuzzy clustering is utilized to supervise level set initialization; second, the object indication function is modified with regard to level set convergence; third, both balloon force and region competition are enhanced to direct level set evolution. All of them may function separately or be unified within a level set formulation for robust segmentation. In particular, it is able to detect and track the arbitrary combination of selected image components. The rest of this paper is organized as follows. Section 2 briefly introduces the common level set formations and their limitations in selective image segmentation. The contributions of fuzzy controlling from initialization, evolution to convergence are elaborated in Section 3. Section 4 reports the experiments and performance evaluation. The last two sections are reserved for discussion and concluding remarks.

II. REGULAR LEVEL SET SEGMENTATION

Image segmentation can be modeled by using a closed interface that separates the image into the region inside the interface and the one outside. LSMs express the interface implicitly by embedding it into a higher-dimensional Lipschitz function

$$\phi(x, y, t) \begin{cases} < 0 & \text{for } (x, y) \in \Omega^- \\ = 0 & \text{for } (x, y) \in \Phi \\ > 0 & \text{for } (x, y) \in \Omega^+, \end{cases} \quad (1)$$

where Φ is an interface separating the image domain Ω , Ω^- denotes the sub-region inside Φ and Ω^+ outside. The dynamic level set function ϕ evolves following the increment t . At any moment T , it is convenient to recover the implicit interface of interest Φ by checking (1), namely $\phi(x, y, t = T) = 0$. Another important advantage of LSMs is that the interface evolution is totally determined by geometrical partial differential equations (PDEs), where various forces are integrated together to advance the dynamic interface toward the optimal sites for image segmentation.

The classical HJ formulation characterizes the interface evolution as [6]:

$$\begin{cases} \frac{\partial \phi}{\partial t} + \mathbf{F} \cdot |\nabla \phi| = 0 \\ \phi(x, y, t = 0) = \phi_0(x, y), \end{cases} \quad (2)$$

where ∇ denotes the operator for geometric gradients, $|\nabla \phi|$ directs the normal orientation for interface evolution, and $\phi_0(x, y)$ defines the initial contour. The velocity field \mathbf{F} consists of the intrinsic forces from the dynamic interface itself (e.g., smoothness and curvature) and the external ones from the image under investigation (e.g., intensity and gradient) and/or other artificial momentums (e.g., balloon forces). For example, (3) characterizes one of the most common HJ-LSMs for level set segmentation, namely geodesic active

contours [27]

$$\frac{\partial \phi}{\partial t} = (\beta\kappa + v)g |\nabla\phi|, \quad (3)$$

where v denotes a constant balloon force, κ the mean curvature, β a controlling parameter that determines whether the dynamic interface shrinks ($\beta > 0$) or expands ($\beta < 0$), and g is the object indication function dependent on the image under investigation; it should be near zero in the object boundaries and positive elsewhere. The object indication function is of vital importance in HJ-LSMs, and also plays a key role in anisotropic diffusion for feature preservation [28].

Mumford and Shah [7] proposed a distinct interface model for image segmentation:

$$F^{MS}(u, \Phi) = \mu \cdot \text{Length}(\Phi) + \lambda \int |\omega - u|^2 dx dy + \int_{\Omega \setminus \Phi} |\nabla u|^2 dx dy, \quad (4)$$

where μ and λ are two controlling parameters, and u is a piecewise smooth approximation of the sub-regions. In essence, (4) pursues an optimal interface, either real or virtual, by minimizing a customized cost function of regional homogeneity. This model can be optimized by a level set formulation [9]

$$\begin{cases} \frac{\partial \phi}{\partial t} = \delta(\phi)[\mu \cdot \text{div}(\frac{\nabla\phi}{|\nabla\phi|}) - \lambda_1(\omega - c_1)^2 + \lambda_2(\omega - c_2)^2] \\ \phi(x, y, t=0) = \phi_0(x, y), \end{cases} \quad (5)$$

where μ , λ_1 and λ_2 are the controlling parameters, c_1 and c_2 are the geometrical approximations of region homogeneity, and $\delta(\phi)$ is the geometrical derivative of Heaviside function.

MS-LSMs are capable of piecewise constant segmentation, but are unfortunately susceptible to image inhomogeneity. It is helpful to restrict competition in every local region [17]

$$\begin{aligned} & \frac{\partial \phi}{\partial t} \\ &= \delta(\phi) \left[\mu \cdot \text{div}(\frac{\nabla\phi}{|\nabla\phi|}) - \left(\lambda_1 \int_{\Omega} \Theta_{\sigma} \left| \omega - \frac{\Theta_{\sigma} * |\omega H(\phi)|}{\Theta_{\sigma} * H(\phi)} \right|^2 \right. \right. \\ & \quad \left. \left. - \lambda_2 \int_{\Omega} \Theta_{\sigma} \left| \omega - \frac{\Theta_{\sigma} * |\omega(1 - H(\phi))|}{\Theta_{\sigma} * (1 - H(\phi))} \right|^2 \right) \right], \end{aligned} \quad (6)$$

or integrate local edge information [30]

$$\frac{\partial \phi}{\partial t} = \alpha \text{div} \left((1 - \frac{1}{|\nabla\phi|}) \nabla\phi \right) + \delta(\phi) \left(\beta \text{div}(\frac{\nabla\phi}{|\nabla\phi|}) + u \right). \quad (7)$$

Here α and β are two customizable controlling parameters. The Gaussian kernel Θ_{σ} in (6) defines a local region that excludes the influence of peripheral inhomogeneity [17]. On the contrary, the anisotropic diffusion term in (7) is able to suppress noise in the piecewise constant regions while preserving object boundaries.

Furthermore, there have been different level set models proposed to integrate both edge and region information for complementary segmentation [16]. They are actually variational models combining boundary, region and shape information

$$\begin{aligned} \frac{\partial \phi}{\partial t} &= g \cdot \left(\text{div}(\frac{\nabla\phi}{|\nabla\phi|}) + \alpha \right) \cdot |\nabla\phi| + \nabla g \cdot \nabla\phi \\ &+ \mu \cdot \text{spf} \cdot \left(\text{div}(\frac{\nabla\phi}{|\nabla\phi|}) + \nu \right) \cdot |\nabla\phi| + \mu \cdot \nabla \text{spf} \cdot \nabla\phi, \end{aligned} \quad (8)$$

where spf denotes a signed pressure force that utilizes both local and global statistical information to control the direction and velocity of the evolving procedure. Meanwhile, the edge information is integrated to facilitate the detection of object boundaries accurately.

III. SELECTIVE LEVEL SET SEGMENTATION

LSMs begin with an initial interface ϕ_0 and proceed toward a locally optimal site ϕ_t that may serve image segmentation. Therefore, the robustness of level set segmentation is subjected to initialization, evolution and convergence. The proceeding example of medical image segmentation demonstrates that it inevitably suffers from the complexity of physiology and pathology. Fuzzy logic provides a good tool dealing with imprecision and incompleteness. An object in fuzzy logic has its membership function varying between 0 and 1; hence it is possible to characterize partial volume effect, partiality of truth and other uncertainties well. Fuzzy c-means (FCM) is one of the most popular algorithms, and has received widespread attention in image segmentation [8], [16]. It attempts to partition a collection of components into C classes, where the components in a same class are as similar as possible, and the ones in different classes are as dissimilar as possible. This philosophy is exactly similar to the region-based level set segmentation that assumes every part of an image should piecewise constant but differ from each other. In other words, there is an intrinsic connection between fuzzy clustering and level set segmentation. It is in essence consistent with mean shift [29] and other mode seeking techniques. Here we attempt to employ fuzzy region competition to enhance LSMs from initialization, evolution to convergence for selective image segmentation.

A. INITIALIZATION

By minimizing a pre-defined cost function

$$J = \sum_x \sum_y \sum_{k=1}^K \mu_k^l(x, y) \|\zeta(x, y) - v_k\|^2, \quad (9)$$

fuzzy clustering may adaptively estimates the centroid of each cluster v_k and the belongingness of every component $\mu_k(x, y)$ to that cluster:

$$\mu_k(x, y) = \frac{\sum_{n=1}^K \|\zeta(x, y) - v_n\|^{2/(l-1)}}{\|\zeta(x, y) - v_k\|^{2/(l-1)}}, \quad (10)$$

$$\nu_k(x, y) = \frac{\sum_x \sum_y \mu_k^l(x, y) \zeta(x, y)}{\sum_x \sum_y \mu_k^l(x, y)}, \quad (11)$$

where $l (> 1)$ is a parameter controlling the fuzziness of segmentation, $\|\cdot\|$ denotes a specific geometric measurement, ζ means a specific trait such as intensity, color, tensor or texture. In this study, without loss of generality, we simply take l equivalent to 2, image intensity as clustering trait and the Euclidean metric for measurement. The algorithm will be optimized when the intensities of image pixels close to their centroid are assigned high membership values, while those that are distinct are assigned low values.

The outcomes $\{\mu_k(x, y) | k = 1, 2, 3, \dots, K\}$ denote the possibility of each image pixel belonging to a specific fuzzy cluster ν_k . In order to figure out a specific object, it is sound to initiate level set evolution ϕ_0 by probabilistic thresholding

$$\phi_0 = 2(\mu_k > \theta) - 1, \quad (12)$$

where θ is customizable between 0 and 1. In practice, a conservative 0.5 works well. Although LSMs are sensitive to initialization, it is contributive to robust level set segmentation by evolving nearby the site of interest. For segmentation of arbitrarily combinational components, it is convenient to identify the selected ones by

$$\phi_0 = 2([\nu_s] > \theta) - 1, \quad (13)$$

where $[\nu_s]$ denotes a subset, namely $\{\nu_s | s \in S \text{ and } S \subset K\}$. It thus leads to

$$\phi_0 = 2(\sum \mu_s > \theta) - 1. \quad (14)$$

B. EVOLUTION

HJ-LSMs and MS-LSMs adopt distinct numerical forces to advance interface evolution. In common HJ-LSMs, there is a constant balloon force σ_0 together with image gradients that either push or pull the dynamic interface. For image segmentation, this constant force has to be modulated by the object indication function so that it is larger in homogeneous regions but turns to zero near boundaries. However, the weak boundaries in medical images are often not sufficient to neutralize the constant balloon force, and the interface eventually leaks away. In contrast, MS-LSMs evolve according to the force of region competition. Chan and Vese [9] proposed a classical formulation like

$$R = \int_{\Omega} \zeta \cdot H(\phi) dx dy - \int_{\Omega} \zeta \cdot (1 - H(\phi)) dx dy, \quad (15)$$

where ζ denotes intensity variance, and $H(\phi)$ is the Heaviside function. It is noteworthy that, due to image noise and/or inhomogeneity, R is often very large and will dominate level set evolution.

A new term is thus proposed for selective region competition

$$R = \sum_{s \in S} \mu_s - \sum_{(j \in K) \cap (j \notin S)} \mu_j, \quad (16)$$

where μ_s , similar to Eq. (14), denotes the selected components of fuzzy clustering, and μ_j denotes the left ones.

This force of fuzzy region competition R varies between -1 and 1 . Its sign determines whether the dynamic interface expands or shrinks. Compared with the common solution (11), this new one enables MS-LSMs to track local objects. In addition, it is also helpful to separate multiple local objects in parallel.

Benefited from fuzzy clustering, a signed balloon force was proposed for HJ-LSMs to drive the interface adaptively toward the object of interest [8]

$$G = [1 - \gamma(2 \sum \mu_s - 1)] \sigma_0. \quad (17)$$

The parameter $\gamma (0 \leq \gamma \leq 1)$ is a balancing factor: if $\gamma = 0$, we have a constant balloon force σ_0 ; if $\gamma = 1$, the balloon force σ_0 is modulated by the selective fuzzy membership function $\sum \mu_s$. The resultant balloon force G is a matrix with a variable pulling or pushing force at each pixel. In other words, the dynamic interface will be attracted towards the object of interest no matter it is outside, inside or lying across the object boundary.

C. CONVERGENCE

MS-LSMSs are advantageous over HJ-LSMSs for quick convergence. In particular, the convergence of the latter is dependent on an object indication function, which is nonetheless discontinuous and not exactly zero. Consequently, boundary leakage is an inherent shortcoming of HJ-LSMs for image segmentation. In order to rectify the weak boundaries, the common object indication function is enhanced for robust convergence

$$E = e^{-10 \max(\eta g_i, (1-\eta)g_\mu)}, \quad (18)$$

where the parameter η balances the contributions of different object indication functions, and the constant 10 is employed to strengthen the convergence of level set evolution. The first term g_i is a normalized edge indicator based on image gradient

$$g_i = \frac{g - \min(g)}{\max(g)}, \quad (19)$$

where g is

$$g = \frac{1}{1 + |\nabla(\Theta * \omega)|^2}. \quad (20)$$

It is derived from the convolution of the image ω with a Gaussian kernel Θ . The second term in (18), g_μ , arises from the selected fuzzy membership functions μ_s . This new object indication function is able to find out an optimal boundary by taking both image information and fuzzy clustering into account.

D. A NEW FORMULATION

A new formulation is proposed to integrate the proceeding solutions together for selective level set segmentation:

$$\begin{cases} \frac{\partial \phi}{\partial t} = \delta(\phi) [\alpha E \cdot G + (1 - \alpha)R] \\ \phi(x, y, t = 0) = \phi_0(x, y), \end{cases} \quad (21)$$

where α is a coordinating parameter, and δ is the Dirac function of the dynamic interface ϕ . It has been proved that, during level set evolution, the interface should keep very close to a signed distance function. Therefore the dynamic interface needs to be re-initialized periodically for the signed distance function. In practice, both geometric diffusion [30] and Gaussian smoothing [11] are found effective in regularizing the dynamic interface, and thus able to eliminate re-initialization. Then it is appropriate to advance the interface evolution like:

$$\begin{cases} \frac{\partial \phi}{\partial t} = \delta(\phi) [\alpha E \cdot G + (1 - \alpha)R] \\ \phi = \Theta * \phi. \end{cases} \quad (22)$$

where Θ is a Gaussian smoothing kernel and $*$ denotes convolution.

The principal steps implementing this level set model for selective image segmentation can be summarized as follows:

1. Conduct FCM.
2. Choose the candidate objects of interest $[\mu_s]$.
3. Compute the enhanced object indication function E as (18) and the signed balloon force G as (17).
4. Initialize the dynamic interface ϕ_0 as (14) and assign it to ϕ .
5. Compute $\nabla\phi$, $\Delta\phi$, $H(\phi)$ and $\delta(\phi)$.
6. Compute the force of fuzzy region competition R as (16).
7. Evolve and regularize the dynamic interface ϕ as (22).
8. If not converging, go back to step 5 and repeat.

IV. EXPERIMENTS

The algorithms were implemented with Matlab® on a ThinkCentre® computer. Unless otherwise specified, the dynamic interface was simply initialized as Eq. (14), the controlling parameters were assigned $\lambda = 5.0$, $\sigma_0 = 2.0$, and $\Delta t = 0.2$. It is possible to tune the coordinating parameters γ (17), η (18) and α (21) for different applications, but they were simply configured 0.5 in default. The iterative evolution of dynamic interface kept going on till it arrived at either of the following conditions, namely 500 times or that the variance of dynamic interface was less than 0.1%.

Rather than the classical HJ-LSM and MS-LSM algorithms, the new formulation was straightforwardly compared with two popular solutions published in [11] and [15], respectively. The first one [11], termed IVC2010 hereafter, is a level set formulation with selective local and global segmentation. It selectively penalizes the level set function to be binary, and then makes regularization by using Gaussian smoothing. There is a parameter α controlling the selection between local and global segmentation. It was assigned 20 without notification in this study. The other formulation [15], termed IVC2013 hereafter, is a level set model enhanced for inhomogeneous image segmentation. It adaptively integrates local and global intensity information to suppress field inhomogeneity. The controlling weight w was adaptively configured according to different images.

A. SINGLE PHASE SEGMENTATION

The first experiment was designed to evaluate the effects of enhancing the object indication function for level set segmentation. Fig. 1 shows an example of cerebral tissue segmentation from an MRI scanning, in which different tissues including white matter (WM), gray matter (GM) and cerebrospinal fluid (CSF) intertwine with each other. In other words, the original scanning (Fig. 1a) is refractory to segment because of severe inhomogeneity and ambiguous boundary. The ordinary edge indicator based on image gradient (Fig. 1e) was not sufficient to control level set evolution (Fig. 1i) in separating WM and GM. Although IVC2010 (Fig. 1j) and IVC2013 (Fig. 1k) took both local and global information into account, they eventually suffered from inhomogeneity and weak boundary. In contrast, the scheme of fuzzy region competition enhanced the object indication functions (Figs. 1f-1h), and made the new formulation effective to separate complex cerebral tissues well (Fig. 1l).

It was evaluated effective for the new formulation to deal with inhomogeneous segmentation in the first experiment. The second one further checked its performance in this regard. Fig. 2a illustrates one of the most famous X-ray images in history, which was also investigated in [15] as an example. The results of fuzzy region competition (Figs. 3b-3c) made it clear that this X-ray hand image was inhomogeneous and challenging for segmentation. IVC2010 did not perform well in dealing with this kind of images (Fig. 2d). In contrast, it was possible to compensate the inhomogeneous field and tune IVC2013 carefully for bone detection and identification (Fig. 2e). Furthermore, the new formulation was not only able to tackle the issues of inhomogeneity and weak boundary, but also able to accomplish the selective segmentation of soft tissues (Fig. 2f).

B. MULTIPHASE SEGMENTATION

There is a geometrical combination in Fig. 3a. It is possible to separate these geometries according to their colors or intensities. The classical MS model, no matter how initialized, was always trapped to the brightest geometries (Fig. 3b). In contrast, the algorithm IVC2010 was able to selectively pick out a part of geometries with different initialization (Fig. 3c). However, the selection was limited to the brightest components only. The algorithm IVC2013 attempted to compensate the intensity difference and eventually reached a suboptimal segmentation (Fig. 3d). Differently, the new formulation was able to pick out the geometries one by one according to their intensities (Figs. 3e-3h). The selective segmentation was illustrated in Fig. 3i. It was a combinatorial segmentation by choosing Figs. 3f and 3h.

The arbitrary combination of selective segmentation was further illustrated in Fig. 4. Fig. 4b contains a map of elasticity reconstructed from the wave image (Fig. 4a) acquired by magnetic resonance elastography (MRE). MRE is a comparatively new technique for functional magnetic resonance imaging (MRI). Different from the regular MRI (Fig. 4c), MRE makes use of elastic shear wave as the probe to

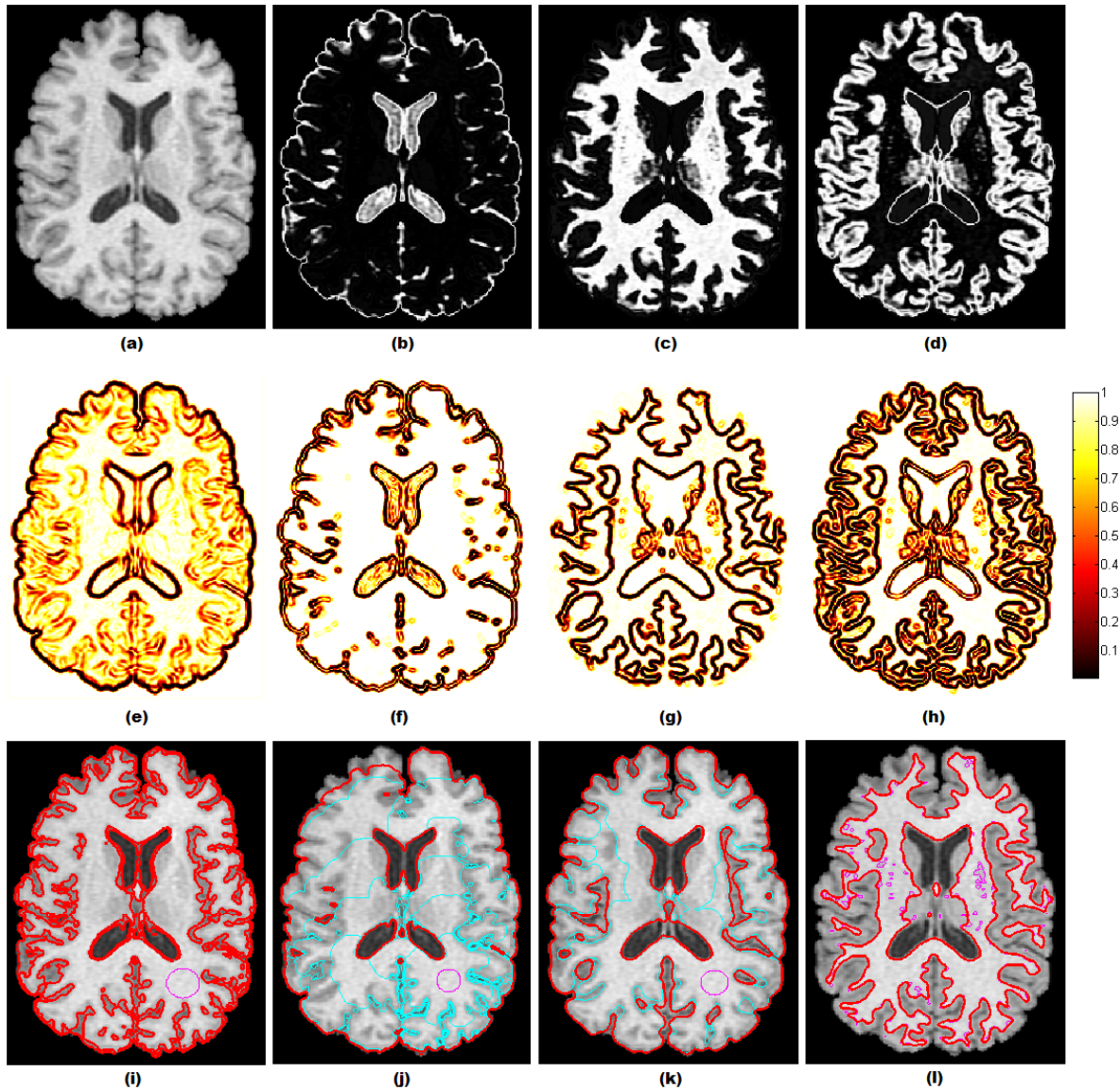


FIGURE 1. Enhancing the object indication functions for cerebral tissue segmentation: (a) MRI cerebral tissues, (b)-(d) probabilistic CSF, WM and GM; (e) the ordinary edge indicator, (f)-(h) the enhanced object indication functions for CSF, WM and GM segmentation; (i) the MS model, (j) IVC2010, (k) IVC2013, and (l) our method.

virtually palpate soft tissues [25]. The information of wave propagation (Fig. 4a) is recorded with a specific MRI pulse sequence [28], and then processed for elasticity reconstruction (Fig. 4b) [31]. Limited by probe resolution and imaging artifacts, the maps of elasticity are currently not as good as their counterparts of relaxation time (Fig. 4c). It thus makes selective level set segmentation challenging. As shown in Fig. 4d, the algorithm IVC2010 was always trapped to the harder tissues (i.e., the darker parts of Fig. 4c but the brighter ones in Fig. 4d) no matter how initialized. Again, the algorithm IVC2013 attempted to compensate the inhomogeneity and eventually reached a non-optimal solution (Fig. 4e). In contrast, only the new formulation was able to carry out the arbitrary combination of selective segmentation, no matter

for the harder components (Fig. 4f) as those by IVC2010 or for the combination of the hardest component and the softest one (Fig. 4h).

Coming to Fig. 5, it is a traditional Chinese painting and full of characteristic freehand components. The preparatory estimation by FCM was effective in detecting the plum blossoms (Fig. 5b), but was not so good at the freehand mountains (Figs. 5c and 5d). The classical MS model was totally dependent on image intensity, and thus sensitive to the inhomogeneity of freehand mountains (Fig. 5e). In contrast, both IVC2010 (Fig. 5f) and IVC2013 (Fig. 5g) were enhanced to track the mountains. They were nevertheless not able to discern the trunks of plum blossom from the freehand mountains. Actually, merely the new formulation

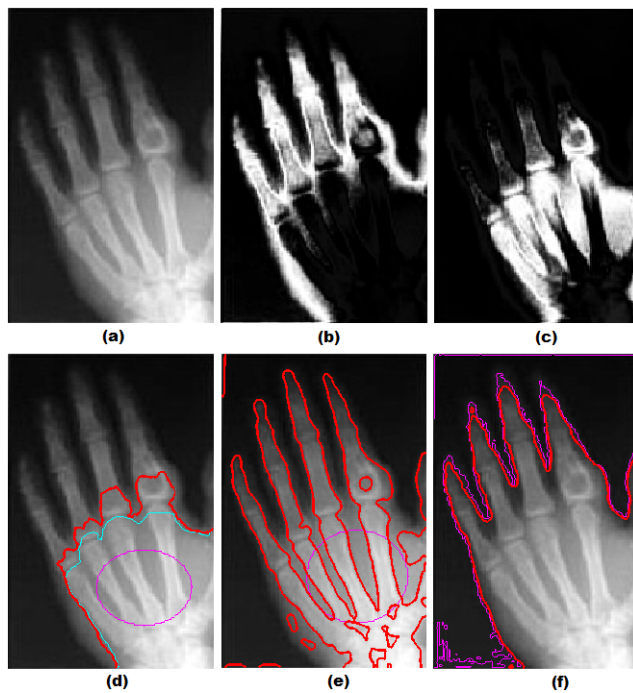


FIGURE 2. Selective segmentation of an X-ray hand image: (a) X-ray hand, (b)-(c) probabilistic estimation by FCM, (d) IVC2010, (e) IVC2013, (f) our method.

was effective in picking the characteristic freehand mountains out (Fig. 5h).

C. QUANTITATIVE SEGMENTATION

Quantitative evaluation was made on two sets of CT liver tumor images. The first dataset (LTS) was taken from the *3D Liver Tumor Segmentation Challenge 2008* (<http://lts08.bigr.nl/>), and consists of 5 CT scans with manually segmented liver tumors by radiologists (Fig. 6a). Another dataset with 5 CT scans (Fig. 6c) was provided by the First Affiliated Hospital of Anhui Medical University (AMU). The radiologists removed all privacy information and demarcated the tumor boundaries.

Both liver and liver tumor segmentation is a grand challenge. For example, it suffers from low contrast for the CT scans in Fig. 6a, and the tumor boundaries are pretty irregular. As shown in Figs. 6b and 6d, the initial results by fuzzy clustering are often unsatisfactory due to noise and artifacts. The new level set formulation was then used for boundary refinement. With area-based metrics, the resultant contours were evaluated against those ground truth boundaries from manual segmentation (Fig. 7).

Assume A_S denotes the detected region and A_T the ground truth, we define the true positive (TP) region by $A_{TP} = A_S \cap A_T$, the false positive (FP) region $A_{FP} = A_S - A_{TP}$, the false negative (FN) region $A_{FN} = A_T - A_{TP}$, and the true negative (TN) region $A_{TN} = (1-A_S) \cap (1-A_T)$. The metrics, including sensitivity (Se) and specificity (Sp), are expressed as follows:

$$Se = \frac{A_{TP}}{A_T}; \quad Sp = \frac{A_{TN}}{A_{TN} + A_{FP}}. \quad (23)$$

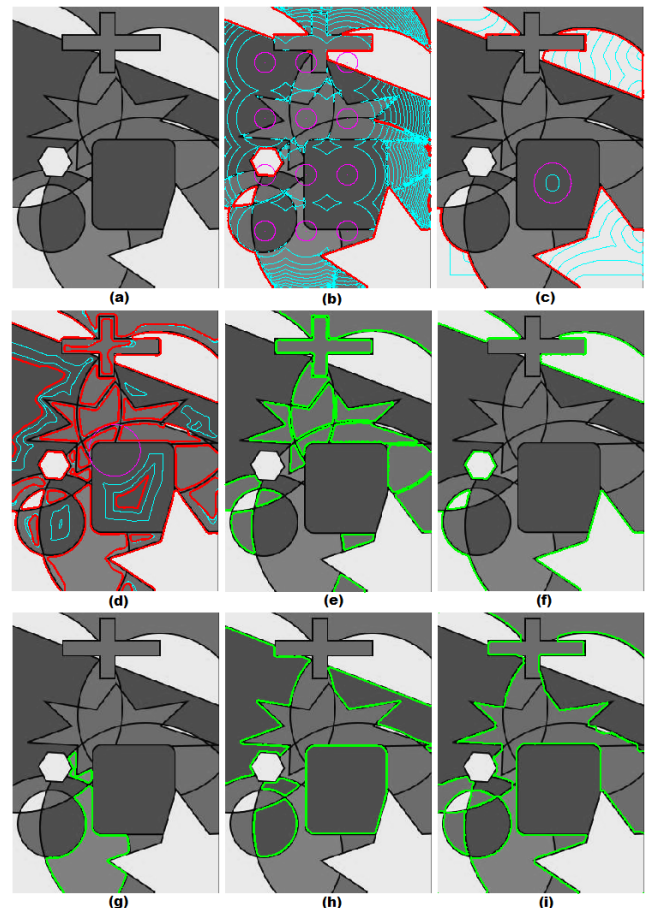


FIGURE 3. Selective level set segmentation of multicolor geometries: (a) Multicolor geometries, (b) the MS model, (c) IVC2010, (d) IVC2013, (e)-(h) selective segmentation, (i) combinatorial segmentation.

Table 1 reports the quantitative performance of the new level set model for liver tumor segmentation. The overall accuracy 84.2% is favorable with respect to the state-of-the-art performance reviewed in [32].

TABLE 1. Quantitative evaluation of liver tumor segmentation.

Dataset	LTS		AMU	
	Se	Sp	Se	Sp
Scan1	0.883	0.989	0.944	0.981
Scan2	0.833	0.993	0.806	0.998
Scan3	0.920	0.989	0.739	1.000
Scan4	0.921	0.994	0.749	1.000
Scan5	0.904	0.991	0.721	0.999
Overall	0.892 ± 0.037	0.991 ± 0.003	0.792 ± 0.091	0.996 ± 0.008

V. DISCUSSION

In LSMs, the HJ models are intrinsically established for selective segmentation. With appropriate initialization and configuration, they are effective to segment any local or global object of interest. The only premise is that there must be outstanding variations or separating boundaries. However, it usually does not hold in most selective segmentation.

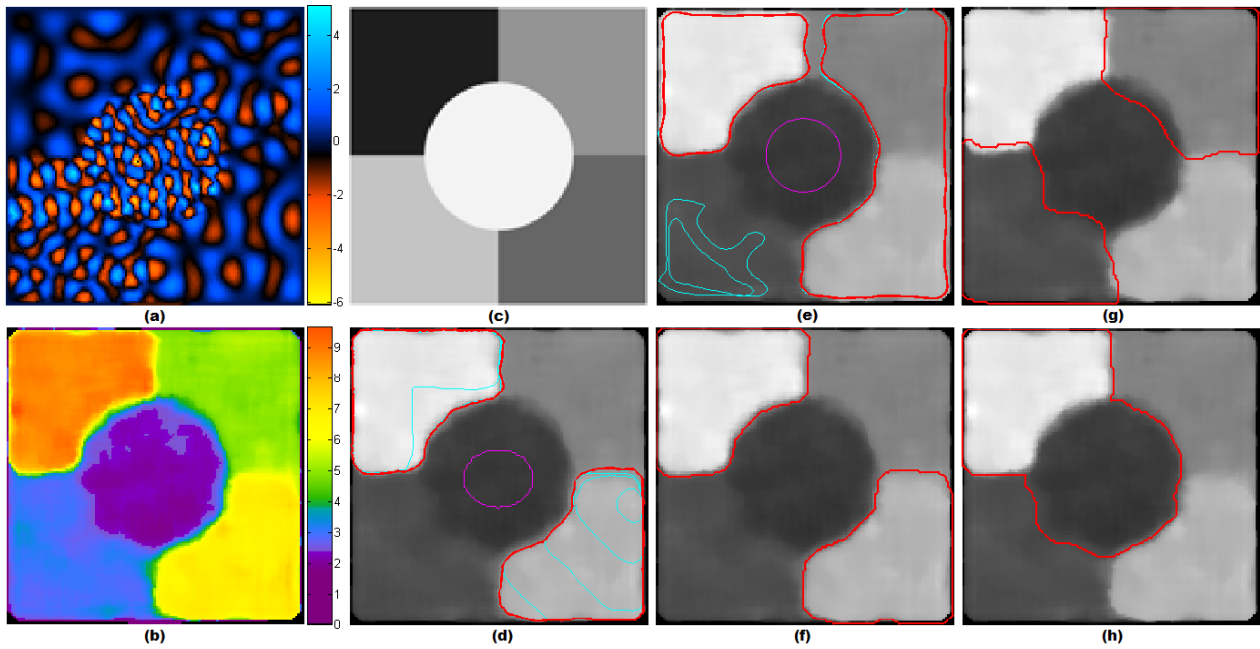


FIGURE 4. Selective MRE segmentation: (a) MRE wave image, (b) map of elasticity, (c) map of relaxation time, (d) IVC2010, (e) IVC2013, and (f)-(h) our method.

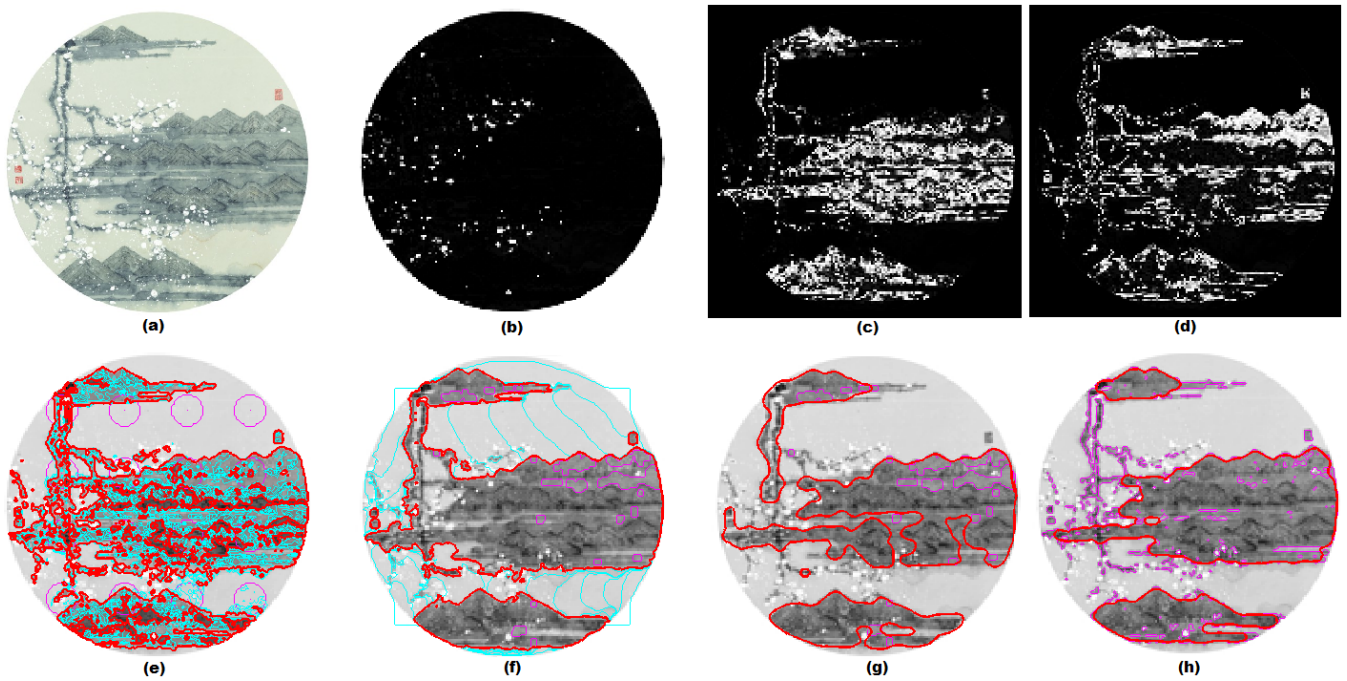


FIGURE 5. Selective level set segmentation of traditional Chinese painting: (a) Chinese painting, (b) probabilistic estimation of plum blossoms, (c)-(d) probabilistic estimation of mountains, (e) the MS model, (f) IVC2010, (g) IVC2013, and (h) our method.

On the contrary, the MS models are made of region competition; hence they are robust to separate the images with weak or even without boundaries. The problem is that they are susceptible to local or non-optimal convergence. It makes this kind of level set models yet ineffective for selective segmentation. The new formulation took advantages

of fuzzy region competition, and was thus benefitted from the enhanced object indication function in the first place (Fig. 1). Other than selective segmentation, it was also capable to pick the arbitrary combination of components or objects out (Figs. 3 and 4), which is usually out of reach for the regular HJ or MS models.

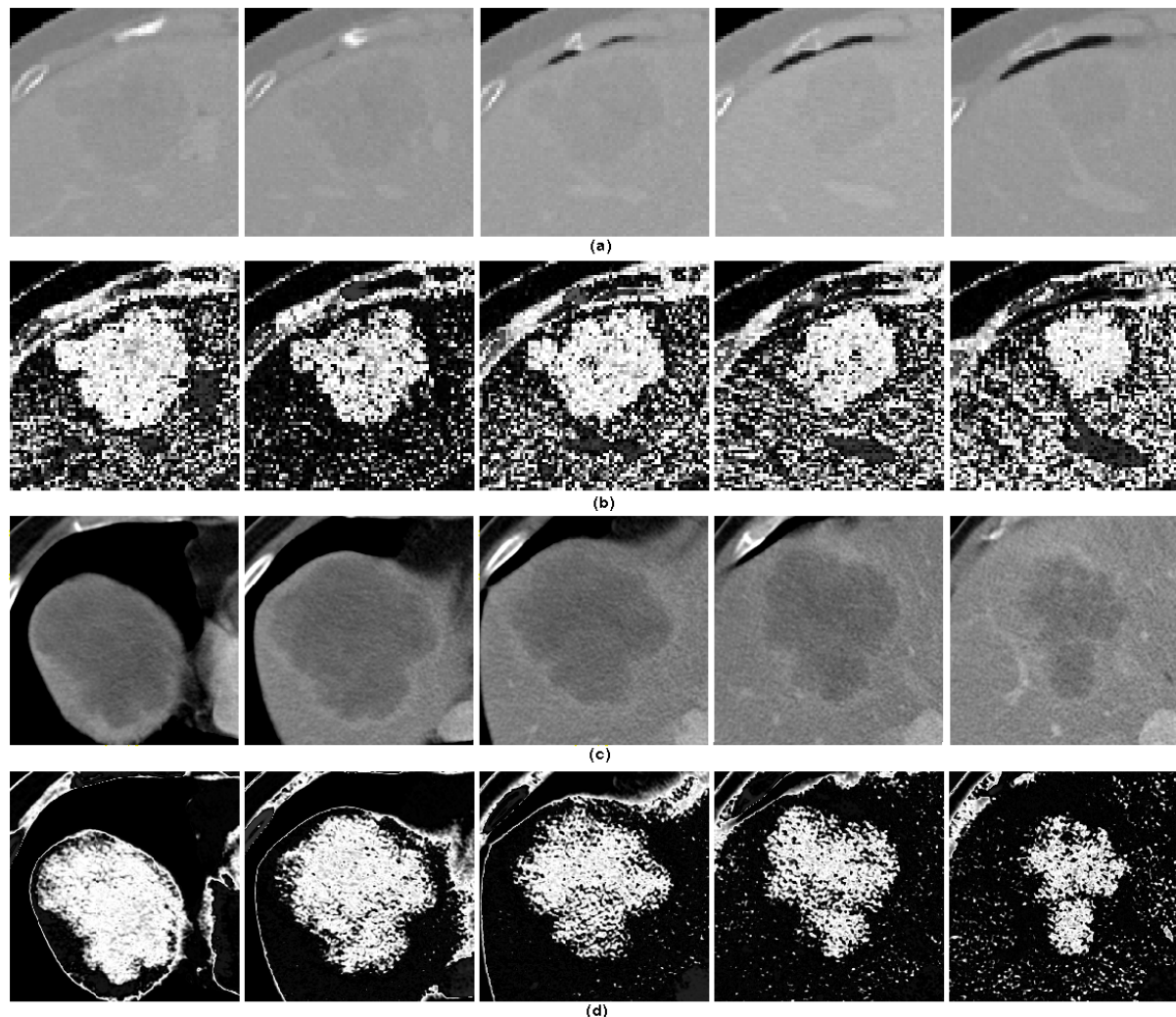


FIGURE 6. Selected CT liver tumor images and the probabilistic distribution of liver tumors by adaptive fuzzy clustering: (a) LTS dataset, (b) liver tumor segmentation by fuzzy clustering; (c) AMU dataset, (d) liver tumor segmentation by fuzzy clustering.

In [11], the algorithm IVC2010 utilized the statistical information inside and outside the desired contour to construct a region-based signed pressure force (SPF) function, which had opposite signs around the object boundary, so the contour shrunk when it was outside the object or expanded when inside the object. It was parametrically controlled for selective local and global segmentation. However, as shown in this study, this algorithm was often trapped to suboptimal solutions. In other words, the performance was substantially dependent on the appropriate initialization. Furthermore, it was not efficient in arbitrary combinations of selective segmentation (Figs. 3 and 4). In contrast, this new model performed well in this regard.

Another big issue in the classical MS models is that they are sensitive to image inhomogeneity [1], [18]. The algorithm IVC2013 in [15] proposed a novel segmentation model integrating the local and global intensity information adaptively in a level set framework. The local region information came from the intensity difference between the averaging

filtered image and the original image. The distance inside each sub-region was minimized that led to the effect similar to piecewise smooth segmentation. However, for multiphase segmentation, the difference might not be owing to object inhomogeneity any more. Instead, it brings many useful hints for selective or combinatorial segmentation. From this point of view, the algorithm IVC2013 might draw misleading conclusions. In contrast, other than selective segmentation, the new formulation was effective in carrying out combinatorial segmentation, which actually made the algorithm robust to image inhomogeneity (Figs. 2 and 5).

In terms of computational efficiency, both algorithms IVC2010 and IVC2013 took advantages of Gaussian smoothing for dynamic interface regularization. It eliminated the need of periodical re-initialization of dynamic interface; hence computational efficiency was improved substantially comparing to that of the regular MS methods (Fig. 8). The new level set formulation inherited this technique to enhance computational efficiency. What is more, benefitted from

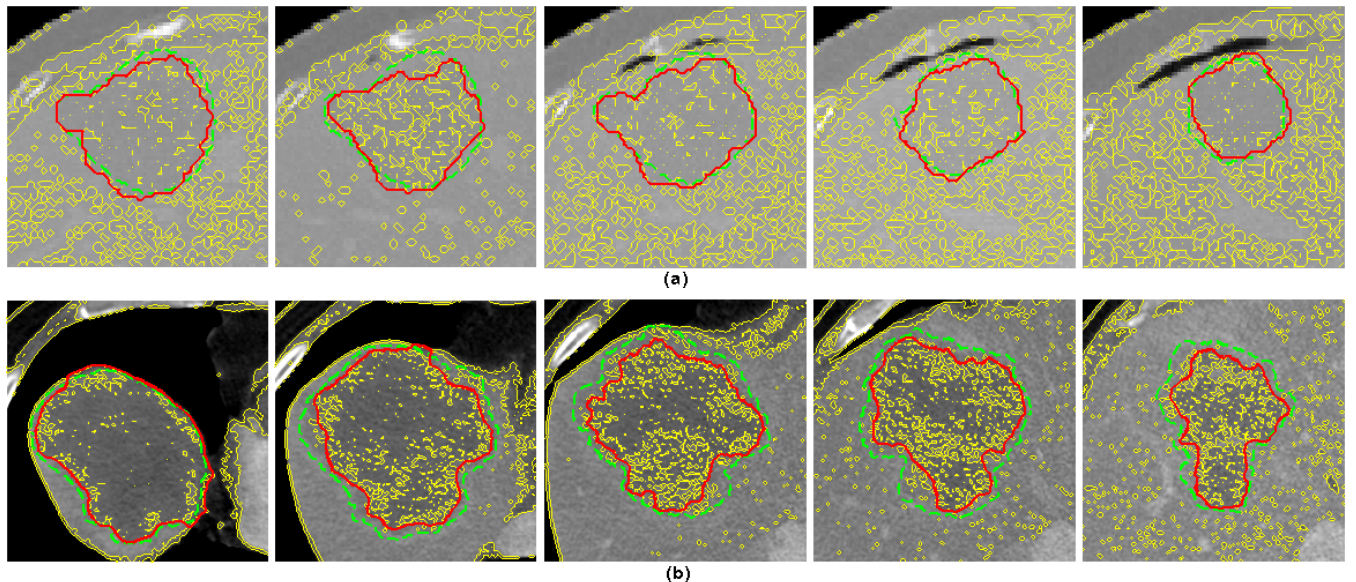


FIGURE 7. Results of liver tumor segmentation by using the new level set formulation: (a) LTS dataset, and (b) AMU dataset. Yellow contours denote fuzzy clustering initialization, green ones denote the ground truth manual delineation, and red ones for level set segmentation.

the preparatory fuzzy region competition, the evolution of dynamic interface usually commences nearby the regions of interest. It thus further promotes the efficiency, which has been well illustrated in Fig. 8. Coming to multiphase segmentation, the new level set formulation is advantageous as well in that the individual selective segmentation runs independently (see III.D). In other words, it is straightforward to parallelize the selective or combinatorial segmentation; hence the performance would be much better than the classical solution in [26].

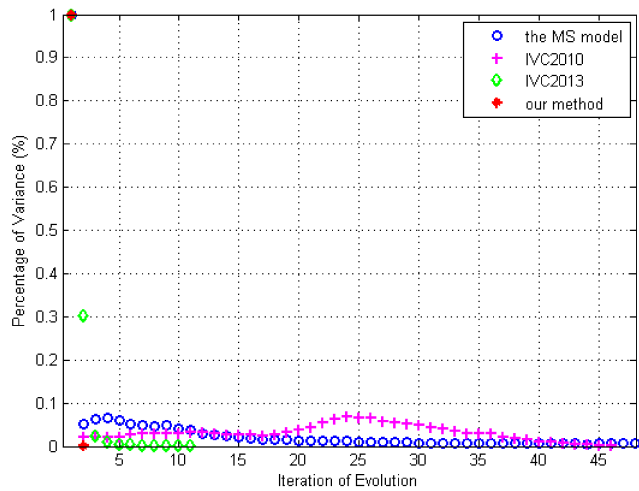


FIGURE 8. Performance evaluation of computational efficiency.

In addition, it is known that common fuzzy clustering is susceptible to noise and artifacts. The results in this study confirmed that the algorithm FCM for fuzzy region competition was indeed sensitive to noise and inhomogeneity, as shown in Figs. 1, 2 and 5. However, in this new level set

formulation, the step of Gaussian smoothing not only controls the regularity of dynamic interface but also effectively suppresses image noise. The dynamic interfaces after level set optimization are smooth and meaningful in contrast to FCM initialization. Actually, level set diffusion has been proposed for noise suppression and image enhancement more than once [19], [28].

Coming to inhomogeneity, it is one of the biggest issues in fuzzy clustering. As shown in Figs. 2 and 5, the algorithm FCM failed to identify the individual components one by one. The new level set formulation is flexible to recombine the selective components for a meaningful segmentation. However, the classical algorithm FCM is totally established on image intensity. It is prone to confusing an object with its background due to local inhomogeneity. If so, the new level set formulation that is controlled by fuzzy region competition would be inefficient for selective segmentation. There have been a variety of techniques proposed to enhance fuzzy clustering for bias correction and inhomogeneity suppression [33]. It is interesting to have those state-of-the-art solutions included for the new level set formulation.

VI. CONCLUSION

There are two well-established level set formulations for image segmentation and shape recovery. However, as shown in this study, both of them have inherent shortcomings when encountering weak boundaries and low contrast. The experiments confirmed that neither gradient-based HJ-LSMs nor region-based MS-LSMs were directly applicable to selective image segmentation. A new level set formulation by using fuzzy region competition was thereby proposed for this purpose. It is able to detect and track the arbitrary combination of selected components or objects. Its performance has been

validated on a series of synthetic and real images. Although this study was established on fuzzy region competition, the new formulation is compatible to Gaussian mixture modeling, Bayesian clustering or other kinds of probability estimating functions for selective level set segmentation.

REFERENCES

- [1] K. Zhang, Q. Liu, H. Song, and X. Li, "A variational approach to simultaneous image segmentation and bias correction," *IEEE Trans. Cybern.*, vol. 45, no. 8, pp. 1426–1437, Aug. 2015.
- [2] C. Scharfenberger, A. G. Chung, A. Wong, and D. A. Clausi, "Salient region detection using self-guided statistical non-redundancy in natural images," *IEEE Access*, vol. 4, pp. 48–60, 2016.
- [3] L. He et al., "A comparative study of deformable contour methods on medical image segmentation," *Image Vis. Comput.*, vol. 26, no. 2, pp. 141–163, Feb. 2008.
- [4] M. Pinheiro and J. L. Alves, "A new level-set-based protocol for accurate bone segmentation from CT imaging," *IEEE Access*, vol. 3, pp. 1894–1906, 2015.
- [5] S. Osher and R. Fedkiw, *Level Set Methods and Dynamic Implicit Surfaces*. New York, NY, USA: Springer, 2003.
- [6] S. Osher and J. A. Sethian, "Fronts propagating with curvature-dependent speed: Algorithms based on Hamilton-Jacobi formulations," *J. Comput. Phys.*, vol. 79, no. 1, pp. 12–49, Nov. 1988.
- [7] D. Mumford and J. Shah, "Optimal approximations by piecewise smooth functions and associated variational problems," *Commun. Pure Appl. Math.*, vol. 42, no. 5, pp. 577–685, Jul. 1989.
- [8] B. N. Li, C. K. Chui, S. Chang, and S. H. Ong, "Integrating spatial fuzzy clustering with level set methods for automated medical image segmentation," *Comput. Biol. Med.*, vol. 41, no. 1, pp. 1–10, Jan. 2011.
- [9] T. F. Chan and L. A. Vese, "Active contours without edges," *IEEE Trans. Image Process.*, vol. 10, no. 2, pp. 266–277, Feb. 2001.
- [10] D. Cremers, M. Rousson, and R. Deriche, "A review of statistical approaches to level set segmentation: Integrating color, texture, motion and shape," *Int. J. Comput. Vis.*, vol. 72, no. 2, pp. 195–215, Apr. 2007.
- [11] K. Zhang, L. Zhang, H. Song, and W. Zhou, "Active contours with selective local or global segmentation: A new formulation and level set method," *Image Vis. Comput.*, vol. 28, no. 4, pp. 668–676, Apr. 2010.
- [12] S. Taheri, S. H. Ong, and V. F. H. Chong, "Level-set segmentation of brain tumors using a threshold-based speed function," *Image Vis. Comput.*, vol. 28, no. 1, pp. 26–37, Jan. 2010.
- [13] M. N. Ahmed, S. M. Yamany, N. Mohamed, A. Farag, and T. Moriarty, "A modified fuzzy C-means algorithm for bias field estimation and segmentation of MRI data," *IEEE Trans. Med. Imag.*, vol. 21, no. 3, pp. 193–199, Mar. 2002.
- [14] D. Smeets, D. Loockx, B. Stijnen, B. De Dobbelaer, D. Vandermeulen, and P. Suetens, "Semi-automatic level set segmentation of liver tumors combining a spiral-scanning technique with supervised fuzzy pixel classification," *Med. Image Anal.*, vol. 14, no. 1, pp. 13–20, Feb. 2010.
- [15] F. Dong, Z. Chen, and J. Wang, "A new level set method for inhomogeneous image segmentation," *Image Vis. Comput.*, vol. 31, no. 10, pp. 809–822, Oct. 2013.
- [16] B. N. Li, C. K. Chui, S. Chang, and S. H. Ong, "A new unified level set method for semi-automatic liver tumor segmentation on contrast-enhanced CT images," *Expert Syst. Appl.*, vol. 39, no. 10, pp. 9661–9668, Aug. 2012.
- [17] C. Li, C.-Y. Kao, J. C. Gore, and Z. Ding, "Minimization of region-scalable fitting energy for image segmentation," *IEEE Trans. Image Process.*, vol. 17, no. 10, pp. 1940–1949, Oct. 2008.
- [18] K. Zhang, L. Zhang, K.-M. Lam, and D. Zhang, "A level set approach to image segmentation with intensity inhomogeneity," *IEEE Trans. Cybern.*, vol. 46, no. 2, pp. 546–557, Feb. 2016.
- [19] A. Tsai, A. Yezzi, and A. S. Willsky, "Curve evolution implementation of the Mumford-Shah functional for image segmentation, denoising, interpolation, and magnification," *IEEE Trans. Image Process.*, vol. 10, no. 8, pp. 1169–1186, Aug. 2001.
- [20] L. Wang, L. He, A. Mishra, and C. Li, "Active contours driven by local Gaussian distribution fitting energy," *Signal Process.*, vol. 89, no. 12, pp. 2435–2447, Dec. 2009.
- [21] Y. Wang, S. Xiang, C. Pan, L. Wang, and G. Meng, "Level set evolution with locally linear classification for image segmentation," *Pattern Recognit.*, vol. 46, no. 6, pp. 1734–1746, Jun. 2013.
- [22] C. Li et al., "Joint probabilistic model of shape and intensity for multiple abdominal organ segmentation from volumetric CT images," *IEEE J. Biomed. Health Informat.*, vol. 17, no. 1, pp. 92–102, Jan. 2013.
- [23] X.-F. Wang, D.-S. Huang, and H. Xu, "An efficient local Chan-Vese model for image segmentation," *Pattern Recognit.*, vol. 43, no. 3, pp. 603–618, Mar. 2010.
- [24] M. Rastgarpour, J. Shanbehzadeh, and H. Soltanian-Zadeh, "A hybrid method based on fuzzy clustering and local region-based level set for segmentation of inhomogeneous medical images," *J. Med. Syst.*, vol. 38, pp. 68–82, Aug. 2014.
- [25] B. N. Li et al., "Modeling shear modulus distribution in magnetic resonance elastography with piecewise constant level sets," *Magn. Reson. Imag.*, vol. 30, no. 3, pp. 390–401, Apr. 2012.
- [26] L. A. Vese and T. F. Chan, "A multiphase level set framework for image segmentation using the Mumford and Shah model," *Int. J. Comput. Vis.*, vol. 50, no. 3, pp. 271–293, Dec. 2002.
- [27] V. Caselles, R. Kimmel, and G. Sapiro, "Geodesic active contours," *Int. J. Comput. Vis.*, vol. 22, no. 1, pp. 61–79, 1997.
- [28] B. N. Li et al., "Evaluation of robust wave image processing methods for magnetic resonance elastography," *Comput. Biol. Med.*, vol. 54, no. 1, pp. 100–108, Nov. 2014.
- [29] P. R. Bai, Q. Y. Liu, L. Li, S. H. Teng, J. Li, and M. Y. Cao, "A novel region-based level set method initialized with mean shift clustering for automated medical image segmentation," *Comput. Biol. Med.*, vol. 43, no. 11, pp. 1827–1832, Nov. 2013.
- [30] C. Li, C. Xu, C. Gui, and M. D. Fox, "Distance regularized level set evolution and its application to image segmentation," *IEEE Trans. Image Process.*, vol. 19, no. 12, pp. 3243–3254, Dec. 2010.
- [31] K. Xiang, X. L. Zhu, C. X. Wang, and B. N. Li, "MREJ: MRE elasticity reconstruction on ImageJ," *Comput. Biol. Med.*, vol. 43, no. 7, pp. 847–852, Aug. 2013.
- [32] T. Heimann et al., "Comparison and evaluation of methods for liver segmentation from CT datasets," *IEEE Trans. Med. Imag.*, vol. 28, no. 8, pp. 1251–1265, Aug. 2009.
- [33] H. Cao, H.-W. Deng, and Y.-P. Wang, "Segmentation of M-FISH images for improved classification of chromosomes with an adaptive fuzzy C-means clustering algorithm," *IEEE Trans. Fuzzy Syst.*, vol. 20, no. 1, pp. 1–8, Feb. 2012.



BING NAN LI (M'11–SM'14) received the B.E. degree in biomedical engineering from Southeast University, Nanjing, China, in 2001, the Ph.D. degree in electronics engineering from the University of Macau in 2010, and the Ph.D. degree in integrative science and engineering from the National University of Singapore in 2012.

He is currently a Full Professor of Biomedical Engineering with the Hefei University of Technology, Hefei, China, and also directs the Center for Magnetic Resonance Imaging X. He has authored over 50 peer-reviewed papers and held over ten patents. His main research interests are healthinformatics and medinformatics, in particular magnetic resonance imaging and computing.

Prof. Li serves on the Editorial Board of the journals *Computers in Biology and Medicine*, *Biomedical Engineering Online*, *Heliyon*, and *Information in Medicine Unlocked*.



JING QIN received the Ph.D. degree in computer science and engineering from the Chinese University of Hong Kong in 2009.

He is an Assistant Professor with the School of Nursing, The Hong Kong Polytechnic University, and also a Key Member with the Centre for Smart Health. He has participated over ten research projects and published over 90 papers in major journals and conferences. His research interests include virtual/augmented reality for health-care and medicine, medical image processing, deep learning, visualization, and human-computer interaction and health informatics.



MENG WANG (M'09) received the B.E. degree from Special Class for the Gifted Young and the Ph.D. degree from the Department of Electronic Engineering and Information Science, University of Science and Technology of China, Hefei, China.

He was an Associate Researcher with Microsoft Research Asia, and then a Core Member in a startup in Silicon Valley. He was with the National University of Singapore, Singapore, as a Senior Research Fellow. He is currently a Professor with the Hefei University of Technology, Hefei. He has authored or co-authored over 100 papers in journals, conference proceedings, and book chapters. His current research interests include multimedia content analysis, search, mining, recommendation, and large-scale computing.

Prof. Wang was a recipient of the best paper award from the 17th and 18th ACM International Conference on Multimedia, the best paper award from the 16th International Multimedia Modeling Conference, the best paper award from the 4th International Conference on Internet Multimedia Computing and Service, and the Best Demo Award from the 20th ACM International Conference on Multimedia.



RONG WANG (M'12) received the B.E. degree in information engineering, the M.E. degree in signal and information processing, and the Ph.D. degree in computer science from the Xi'an Research Institute of Hi-Tech, Xi'an, China, in 2004, 2007, and 2013, respectively, and the Ph.D. degree from the Department of Automation, Tsinghua University, Beijing, China, in 2013.

His current research interests include signal processing and machine learning, together with their applications, such as pattern recognition, image processing, and computer vision.

XUELONG LI (M'02–SM'07–F'12) is a Full Professor with the Center for OPTical IMagery Analysis and Learning, State Key Laboratory of Transient Optics and Photonics, Xi'an Institute of Optics and Precision Mechanics, Chinese Academy of Sciences, Xi'an, China.

• • •